

Additional contributions to CMIP5 Regional Sea Level Projections resulting from Greenland and Antarctic Ice Mass Loss

N. Agarwal^{1,4}, J. Jungclaus¹, A. Köhl², C.R. Mechoso³, and D. Stammer²

¹ Max Planck Institut für Meteorologie, Hamburg, Germany

² Centrum für Erdsystemforschung und Nachhaltigkeit (CEN), Universität Hamburg, Germany.

³ Dept. Atmospheric and Oceanic Sci., U. California Los Angeles (UCLA), Los Angeles, CA, U.S.A.

⁴ Current affiliation: Atmospheric and Oceanic Sciences Group, Space Applications Centre, Ahmedabad, India

E-mail: neeraj@sac.isro.gov.in

Abstract. The impact of Greenland and Antarctic ice sheet mass loss on regional sea level is evaluated here under RCP 4.5 and RCP 8.5 scenarios for the period 2081-2099. To this end, estimates of associated fresh water sources are added to the Max Planck Institute for Meteorology's Earth System Model (MPIESM) ocean component and the dynamical impact is quantified in terms of the difference in sea level relative to previous CMIP5 runs. Overall, the addition of these freshwater sources have only a small impact on regional sea level variations relative to the global mean (<2cm in magnitude). However, in some regions, notably in the North Atlantic and Arctic Ocean, an additional increase in regional steric sea level by 4-8 cm can be obtained, which is ~20% more than the previous climate model response. Climate feedbacks can have additional sea level impacts regionally, e.g., through changes in the wind forcing or surface freshwater fluxes. Overall, the dynamical regional sea level response to the polar ice mass loss is of the same order as the simulated decadal sea level variability.

1. Introduction

Climate projections suggest that on regional scales the increase of sea level at the end of the 21st century can deviate substantially from a global mean value (see Perrette et al. [2013] and for a recent estimate Slangen et al. [2014]). This will hold especially in coastal regions of the western North Atlantic Ocean and Antarctic Circumpolar Current, where sea level rise by the end of the century could be higher by 30% than the global average [Carson et al., 2014]. In contrast, the sea level rise of the subpolar North Atlantic Ocean, Arctic Ocean and off the western Antarctic coast will likely reach only 50% of the global mean; in the vicinity of declining polar ice sheets sea level can even drop with respect to

36 the present day levels. These estimates are based on projections resulting from the Phase
37 5 of the Coupled Model Intercomparison Project (CMIP5; Taylor et al. [2012]; simulating
38 sea level changes associated with a changing ocean circulation and with an increased
39 oceanic heat uptake) combined with off-line (i.e., not part of the CMIP5 runs) estimates
40 of regional sea level rise resulting from changes of land ice, groundwater depletion and
41 glacial isostatic adjustment (GIA). However, substantial uncertainties remain in these
42 estimates, partly due to both internal variability in the individual CMIP models and to
43 shortcomings in our understanding of underlying processes.

44 Uncertainties in regional sea level projections can also result from hitherto neglected
45 processes in the climate models such as the freshwater input originated by glacier and
46 polar ice sheet mass loss. Stammer [2008] demonstrated that the ocean circulation will
47 adjust regionally and dynamically to this addition of extra freshwater through steric
48 processes, while Stammer et al. [2011] suggested that an associated response of the
49 coupled ocean-atmosphere system will lead to additional non-local sea level changes
50 through faster atmospheric teleconnections, which was further investigated by Agarwal
51 et al. [2014]. However, these previous studies were based on idealized freshwater input
52 functions and do not provide quantitative estimates on the uncertainty in existing
53 CMIP5 results originating from the neglect of any freshwater sources from glacier and
54 ice sheet mass loss. Recently, van den Berk and Drijfhout [2014] assessed the impact of
55 a high-end scenario of polar ice loss on a RCP8.5 scenario run of a CMIP5 model. Their
56 assessment was based on prescribing a large mass loss from Antarctica of nearly 50 cm
57 equivalent sea level rise and produced the largest impact on the Antarctic continental
58 shelf. The extent to which this result is representative of CMIP type models under
59 realistic conditions remains unclear.

60 The aim of this paper is to quantify the amplitude of an additional regional sea
61 level change at the end of the 21st century that would result dynamically in a moderate
62 (RCP 4.5) and a high-end (RCP 8.5) climate projection, respectively, if realistic local
63 freshwater sources from retreating land ice masses were added to the model oceans.
64 In this study we restrict our attention initially to water sources from Greenland and
65 Antarctic only, while the contribution from continental glaciers is currently ignored due
66 to the difficulties in prescribing glacier locations and associated hydrology for the melted
67 water. We will argue below, however, that all cryospheric freshwater sources need to be
68 added to future CMIP models to properly address the important question of regional
69 sea level projections.

70 **2. Methodology**

71 All experiments analyzed in the present study use the low-resolution configuration of
72 the Max Planck Institute for Meteorology Earth System Model (MPI-ESM), which was
73 run under the CMIP5 protocol [Giorgetta et al., 2013]. The MPI-ESM model is a fully
74 coupled Earth system model; however, it does not include land ice sheets and land
75 glaciers. Hence the climate change feedbacks arising due to net mass loss of ice and

76 glaciers are not included [Jungclaus et al., 2006].

77 The MPI-ESM RCP 4.5 and RCP 8.5 simulations from the period 2006-2099 are
78 our reference runs for each climate change scenario. Simulations were repeated under
79 both scenarios starting in 2006, but now including additional time-dependent freshwater
80 sources representing the mass loss of Greenland and Antarctic ice sheets (GIS and
81 AIS, respectively) as projected during AR5. The differences between simulated results
82 with and without the additional sources serve as the basis for our analysis. Present-
83 day mass loss rates of GIS and AIS for 2006 are estimated to be 250 Gtyr⁻¹ and 81
84 Gtyr⁻¹, respectively [Shepherd et al., 2012]. Starting from these values, time series
85 of annual mean mass loss rate projections were constructed for the period 2006-2099
86 for both RCP 4.5 and RCP 8.5, which are consistent with recent AR5 global sea level
87 change projections obtained by using surface mass balance models and ice dynamical
88 contributions (J.M. Gregory, personal communication; see also [Church et al., 2013]).
89 The upper panel of Fig. 1 shows the resulting mass loss rates separately for GIS and Fig. 1
90 AIS and for RCP 4.5 and RCP 8.5. On global average, these values add up to 16 cm
91 and 20 cm respectively for RCP4.5 and RCP8.5 scenarios and are consistent with AR5
92 estimates (7 - 17 cm and 12 - 24 cm for RCP4.5 and RCP8.5, respectively). Helm et al.
93 [2014] critically discussed the differences in their mass loss estimates of 2011-2014 with
94 those obtained by Shepherd et al. [2012], which we have used in our study. We used the
95 values of 250 Gtyr⁻¹ and 81 Gtyr⁻¹ for the starting year 2006 (start of CMIP5 runs).
96 If we estimate the mass loss rates of 2014 from our Fig. 1 (upper panel) it comes out to
97 be 320 Gtyr⁻¹ and 100 Gtyr⁻¹ making a combined loss of 420 Gtyr⁻¹ which is quite
98 close to the estimates given by Helm et al. [2014].

99 According to Fig. 1, mass loss rates for GIS reach up to 700 Gtyr⁻¹ and 1400
100 Gtyr⁻¹ by the end of the 21st century for RCP 4.5 and RCP 8.5, respectively. For
101 AIS, the mass loss rates under RCP 4.5 reach 250 Gtyr⁻¹ by the end of the century
102 while under RCP 8.5 these value initially increase, but decline after 2050 to around
103 zero in 2097, after which they rise again. The decline in mass loss rates after 2050 is
104 consistent with the AR5 report (upper panel Fig. 1). Church et al. [2013] updated
105 the records (shown in the upper panel of Fig.1 as dashed lines) , which led to changes
106 mainly in the estimates for the RCP4.5 scenario. The AR5 authors point, however, to
107 large uncertainties. We therefore consider the differences between the estimates by J.M.
108 Gregory (personal communication) that we used in our study and the ones published in
109 AR5 small and don't expect any significant change in our results due to this difference.

110 The associated freshwater input we prescribe into the model ranges from about
111 0.011 Sv to 0.022 Sv for RCP 4.5, and from 0.015 Sv to 0.05 Sv for RCP 8.5. Around
112 Greenland the prescribed melt water flux was applied uniformly in space. For Antarctica
113 the freshwater source was applied only around the West-Antarctic ice sheet. No source
114 was prescribed around Eastern Antarctica, which has experienced mass gains in recent
115 years [Shepherd et al., 2012]. In their study, van den Berk and Drijfhout [2014] used
116 the outputs from iceberg drift model. However, since these outputs were not available
117 to us, we use fixed patterns of runoff adjacent to the continents following Swingedouw

118 et al. [2013].

119 The experiments with additionally applied net mass loss rates due to polar ice
120 sheet melting (PIM) are referred to hereafter as RCP4.5+PIM and RCP8.5+PIM,
121 respectively. For each scenario, an ensemble of three member simulations was performed
122 similarly to CMIP5. The results are discussed in the next section in terms of the
123 difference between the ensemble means of the runs with PIM minus the simulations
124 without PIM and will be referred to as E4.5 and E8.5, respectively.

125 We note for the later interpretation of results that under both climate scenarios the
126 prescribed time-varying and slowly increasing freshwater forcing is substantially lower in
127 amplitude than in Stammer et al. [2011], who used a constant forcing of 0.0275 Sv for the
128 entire 50 year period of their study. Only during the last 20 years of RCP8.5+PIM does
129 our monotonically increasing forcing becomes comparable to the one used by Stammer
130 et al. [2011]; for RCP4.5+PIM it is always less. The resulting differences in freshwater
131 input are reflected in the differing global mean sea level rise, which in our case range
132 between 16 and 20 cm over a 100 - year period (Fig. 1b). By contrast, the global mean
133 sea level rise in Stammer et al. [2011] reached an amplitude around 11 cm within 50
134 years. In comparison to van den Berk and Drijfhout [2014], the total applied freshwater
135 forcing in our scenario runs is about a factor 3-4 smaller; the input around Antarctica
136 is in fact more than a factor of 10 smaller.

137 **3. Results**

138 The lower panel of Fig.1 presents time series of global mean sea level differences
139 (see definition in the previous section) corresponding to E4.5 and E8.5, respectively.
140 This figure shows an increase in global mean sea level of about 17 cm and 21 cm
141 in RCP4.5+PIM and RCP8.5+PIM, respectively. We note that in either case, the
142 increase is about 1 cm higher than expected from the prescribed mass loss rates alone,
143 a differences that emerges from additional surface freshwater flux related to climate
144 feedbacks. The additional increase in sea level is similar to one that was discussed in
145 Stammer et al. [2011] where the GIS meltwater caused an additional increase in sea level
146 anomaly.

147 All effective sources of freshwater (direct and indirect) are summarized in Table 1 Table 1
148 showing the direct freshwater discharge from AIS and GIS, together with the indirect,
149 freshwater input resulting from aggregated differences in the net surface freshwater fluxes
150 that take into account changes in evaporation minus precipitation over the ocean and
151 river run-off. Relative to the discharge from AIS and GIS, however, the magnitude of
152 the latter terms amounts to just a few percent.

153 To illustrate how the net freshwater volume added in high latitudes of the Atlantic
154 and in the Southern Ocean is redistributed by the ocean circulation during the 100 year
155 projection, Table 1 shows the space-time-mean freshwater content differences integrated
156 over individual ocean basins (Pacific, North and South Atlantic, Arctic, Southern and
157 the Indian Ocean) averaged over the period 2081-2099. According to the table, less

158 than 50% of the freshwater amount added around Greenland remains in the region
159 in E4.5, while 20% moves into the Arctic. The amount accumulated in the Southern
160 Ocean is more than double that of the freshwater added locally by AIS, indicating that
161 a significant amount of freshwater got redistributed to other parts of the world oceans.

162 We note that in contrast to E4.5, in which about 40% of the net freshwater input
163 ends up in the Pacific Ocean, In E8.5 the Pacific is losing freshwater, however, in
164 all regions (except in the North Atlantic) intra-ensemble deviations in circulation are
165 substantial which does not allow for firm conclusions on scenario differences with our
166 limited samples. The largest impact is expected from changes in the surface fluxes. The
167 small size of the ensemble simulations does not allow us to carry out a quantitative
168 uncertainty assessment in the results (see also discussion in Section 4).

169 As can be expected from previous results of Stammer et al. [2011], perturbing the
170 coupled system by meltwater perturbation can lead to feedback mechanisms that will
171 alter the surface fluxes of momentum (wind stress), heat, and even freshwater itself.
172 The left column of Fig. 2 shows the respective ensemble mean of net surface freshwater
173 fluxes changes in response to the additional freshwater forcing of the ocean. The
174 largest changes occur over the tropical Pacific and Indian Ocean region. However, the
175 comparison with the level of decadal variability of the pre-industrial control run shows
176 only a few regions with values well beyond the system's internal variability (see also
177 Fig. S1 in the supplementary material for similar differences from individual ensemble
178 members).

Fig. 2

179 The right column of Fig. 2 shows the ensemble mean differences in zonal wind stress
180 from E4.5 and E8.5 over the period 2081-2099 (see also Fig. S2 in the supplementary
181 material for similar differences from individual ensemble members). For E4.5, the
182 westerly zonal wind stress is reduced in the subpolar region south of Greenland and
183 increased in the subtropical North Atlantic. Similarly, in the Southern Ocean around
184 60°S, the westerly zonal wind stress is reduced. By contrast, E8.5 shows an increase
185 in westerly zonal wind stress in the subpolar region south of Greenland and also in the
186 Southern Ocean centered at 40°S between 50°W and 100°E. South of Greenland these
187 results of E8.5 are similar to those of Agarwal et al. [2014] who reported a strengthening
188 of westerlies as a part of the early response to the net mass loss from the GIS. However,
189 the weakening of westerly zonal wind stress in E4.5 is not in agreement with Agarwal
190 et. al. (2014). One of the reasons for this could be the reduced strength of freshwater
191 flux from GIS in case of E4.5. Furthermore, in E4.5 the negative anomaly south of
192 Greenland was found to be a part of long-term (20 years) internal variability of the
193 system. Particularly at higher latitudes, internal variability has been found to be large
194 for sea level pressure and can easily obscure regional differences in projections [Deser
195 et al., 2012].

196 To provide an estimate of dynamical sea level changes missing in CMIP5 results
197 due to the lack of freshwater source from polar ice mass loss, the left panels of Fig. 3
198 show the regional sea level in E4.5 (see also Fig. S3 in the supplementary material for
199 similar differences from individual ensemble members). The values in the top panel of

Fig. 3

200 Fig. 3 correspond to the sea level changes (dynamical + global mean steric) between
201 experiments with and without PIM. Sea level changes are mostly positive in the northern
202 hemisphere, notably in the North Atlantic and the Arctic. In the North Atlantic and
203 Nordic Seas the steric sea level increase in response to Greenland ice mass loss can
204 be around 2-4 cm; however, the changes are substantially larger in the Arctic Ocean,
205 thus enhancing the already large sea level rise there (compare Fig. 4). In contrast, Fig. 4
206 positive sea level differences in the southern hemisphere are restricted to the immediate
207 vicinity of the Antarctic continent; this holds also for the eastern Antarctic region where
208 no perturbation was directly applied. Most of the remaining Southern Ocean, however,
209 shows negative sea level changes relative to the global mean increase, which is consistent
210 with the pole-ward shift in zonal wind stress described above and associated shift in the
211 position of the Antarctic Circumpolar Current (ACC) as described by Fyfe and Saenko
212 [2006]

213 In E8.5, the sea level increase in the North Atlantic and in the Nordic Seas ranges
214 between 0.5 and 2 - 4 cm, with higher values mainly in the Labrador Sea and in the
215 subpolar and subtropical gyre regions. Despite the stronger freshwater input from
216 Greenland, the sea level differences in the Arctic Ocean are weaker compared to E4.5
217 suggesting that the changes are likely due to climate variability rather than indicating
218 a causal connection to the freshwater input.

219 The middle and bottom rows of Fig.3 display the thermosteric and halosteric
220 contributions to sea level changes, respectively. As can be expected, changes in the
221 North Atlantic and Nordic Seas are mainly due to the halosteric component. The
222 largest increase (around 10 cm) is in the southeast edge of subtropical gyre; however this
223 increase is compensated by a decrease in the thermosteric component and is probably
224 related the subduction of salinity differences. Note that the associated changes in
225 spiciness also imply changes in subducted temperature anomalies. Due to the change in
226 thermal expansion to haline contraction ratio along the subduction path, temperature
227 differences will grow [Tailleux et al., 2005], which explains the stronger thermosteric
228 signal at the southern edge. In summary, in the North Atlantic, changes in the total
229 and the components of the steric sea level response are similar in the two scenarios.

230 Along with the freshening of the North Atlantic, we diagnose a decrease in surface
231 salinity in both E4.5 and E8.5 (SSS; not shown). Due to stronger mass loss rates in E8.5,
232 the averaged SSS differences for the period 2081-2099 are larger in the North Atlantic.
233 In contrast to van den Berk and Drijfhout [2014], in the regions where net mass loss
234 from Antarctic is applied, both E4.5 and E8.5 show very little response in agreements
235 with the weaker freshwater input. Sea Surface Temperatures (SST) are lower around
236 Greenland in both scenarios, and in the subpolar gyre in E8.5 (not shown). A cooling
237 in the subtropics can only be seen in E4.5; however, there are negative SST differences
238 in Southern Ocean near the western Antarctic Peninsula. E8.5 also obtains negative
239 differences in the South Atlantic.

240 In the North Atlantic we observe an increase in the halosteric component due to the
241 increase in freshwater content and simultaneous decrease in the thermosteric component

242 due to decrease in heat content. For E8.5, this results in a net change of around 2 cm
243 in sea level by the end of the century. Since the amount of freshwater released in
244 the North Atlantic is larger in E8.5 than in E4.5, one could have expected a larger
245 difference between the experiments in terms of sea level change. However, although, the
246 halosteric sea level change is in fact around 2 times larger in E8.5, the net effect on sea
247 level is reduced due to a compensating effect created by a decrease in the thermosteric
248 component. In most others locations, differences have very small magnitudes.

249 To quantify the relative contributions from halosteric and thermosteric changes to
250 the net steric sea level changes, Table 2 shows for each ocean basin separately the sea
251 level differences and their halo-steric and thermo-steric contributions as basin averages.
252 In both E4.5 and E8.5, the maximum change in sea level is in the North Atlantic
253 and Arctic Oceans (~ 2 cm). We note, however, that for E8.5 in the North Atlantic
254 an increase in the halosteric component (due to increased freshwater content) and a
255 simultaneous decrease in the thermosteric component (due to decreased heat content)
256 results in a net change of around 2 cm in sea level by the end of the century. In E4.5,
257 the maximum change is mainly due to the halosteric component. Since the amount of
258 freshwater released in the North Atlantic is larger in E8.5 than in E4.5, one could have
259 expected a larger impact in terms of sea level change. However, although the halosteric
260 sea level change is in fact around 2 times larger in E8.5 than in E4.5, the net effect on sea
261 level is reduced due to a compensating effect created by a decrease in the thermosteric
262 component. In most other regions the dynamical effects on regional sea level projections
263 due to polar ice sheet mass loss appear insignificant.

264 During the first 60 years, the total steric change in the North Atlantic is around
265 zero (not shown); during the following years, however, sea level rises steadily with long
266 term oscillations superimposed. In contrast, sea level in the Arctic Ocean rises from the
267 beginning of the experiments with a steepened increase starting from 2070 to 2090 to be
268 followed by a slight decrease towards the end of the century. There is a slight increasing
269 trend in sea level in the South Atlantic beginning from year 2030, however the changes
270 are quite small (1cm). In other regions, changes in sea level are negligible and remain
271 within the natural long term variability. To further quantify the relative impact of the
272 impact of freshwater input, the left panels in Fig.4 show the percentage change in steric
273 sea level for both E4.5 and E8.5 scenarios during 2081 - 2099 after normalization with
274 the changes 2081 - 2099 minus 1986 - 2005 of the MPI-ESM for RCP4.5 and RCP8.5,
275 respectively. The ensemble mean sea level changes (in cm) from RCP4.5 and RCP8.5
276 are shown in the right panels as reference.

277 For RCP4.5 forcing, the maximum relative changes due to net mass loss rates from
278 GIS and AIS appear in the North Atlantic and in the Arctic regions. In the regions
279 around the coast of Greenland and north-east of North America, changes in sea level
280 are up to 20% while in the Eurasian Basin of the Arctic the sea level increase is more
281 than 20%. The changes in the subpolar and subtropical North Atlantic are between 2 -
282 4%. In the Southern Ocean, the changes in sea level are less than 10%. In E8.5, changes
283 in sea level are between 10 - 20% around Greenland and in the Eurasian Basin of Arctic

Fig.4

284 Ocean. Elsewhere, changes in sea level are less than 5%. The changes in subtropical
285 North Atlantic are similar in the two experiments. There is a slight increase in sea level
286 in the North Western Pacific; changes in the Southern Ocean remain small except in
287 the sector 50°E - 80°E.

288 **4. Conclusions**

289 The goal of this paper is to provide a quantitative assessment of the amplitude of regional
290 sea level changes at the end of the 21st century that would result dynamically in RCP
291 4.5 and RCP 8.5 climate projections from previously missing local freshwater sources
292 around retreating land ice masses. We recall that in this pilot study only the mass loss
293 of polar ice sheets is considered. We therefore have to keep in mind that differences
294 shown here are likely to be at the lower end of what will result from future CMIP runs
295 with all melt water sources included.

296 The regional impact of the missing sources stays mostly below 2 cm with largest
297 values not exceeding 10 cm. We note that this signal is a factor 2-3 times smaller
298 in comparison to the recent study by van den Berk and Drijfhout [2014], who used a
299 stronger forcing. We also find a weaker impact in the North Atlantic and Arctic Ocean
300 as well as along the Antarctic shelf. The difference in the regions close to the Antarctic
301 coast are negligible in magnitude, but are overall negative in the Southern Ocean.

302 The number of simulations in our ensembles are the same as in the CMIP5 runs of
303 the model. Our estimate of statistical significance is based on a comparison with internal
304 variability in the unforced control simulation. However, for an improved assessment of
305 how robust our results are on regional scales, a substantially larger ensemble size would
306 be needed. In an attempt to show systematic behaviors the supplementary material
307 presents similar changes of surface freshwater and wind stress fluxes as well as those for
308 net sea level for each member of the ensembles. Variability between ensemble members
309 is inevitable as was highlighted recently by Deser et al. [2012] and by Hu and Deser
310 [2013] in terms of sea level.

311 Although our results suggest a small additional sea level signal which renders the
312 current sea level changes mostly unaffected, regionally larger contributions of up to 20%
313 exist implying that in future quantitative CMIP-type projections glacier mass loss has
314 to be considered simultaneously with polar ice sheet mass loss and both effects should
315 be build into climate models to include all components of regional sea level changes.
316 Furthermore, substantially large ensemble size estimates are required for more accurate
317 regional sea level change projections in any CMIP based analyses.

318 **Acknowledgments**

319 This work was funded in part through a Max Planck Society (MPG) Fellowship
320 awarded to D. Stammer, through the BMBF (Federal Ministry of Education and
321 Science) funded Project RACE, through the EU-funded NaCLIM project, and through

322 the CliSAP Excellence Cluster of the University of Hamburg, funded through the
323 Deutsche Forschungsgemeinschaft (DFG). Additional funding was provided by the
324 National Science Foundation grant AGS 1041477 at UCLA. Contribution to the CliSAP
325 Excellence Cluster, also funded through the DFG.

326 **References**

327

328 N Agarwal, A Köhl, C R Mechoso, and D Stammer. On the early response of the climate
329 system to a meltwater input from greenland. *Journal of Climate*, 27(21):8276–8296,
330 2014.

331 M Carson, A Köhl, and D Stammer. The impact of regional multidecadal and century-
332 scale internal climate variability on sea level trends in cmip models. *Journal of*
333 *Climate*, (2014), 2014.

334 J Church, PU Clark, et al. Chapter 13: Sea level change. *Working Group I Contribution*
335 *to the IPCC Fifth Assessment Report, Climate Change 2013: the Physical Science*
336 *Basis*, 2013.

337 C Deser, A Phillips, V Bourdette, and H Teng. Uncertainty in climate change
338 projections: the role of internal variability. *Climate Dynamics*, 38(3-4):527–546, 2012.

339 J C Fyfe and O A Saenko. Simulated changes in the extratropical southern hemisphere
340 winds and currents. *Geophysical Research Letters*, 33(6), 2006.

341 M A Giorgetta, J Jungclaus, C H Reick, S Legutke, J Bader, M Böttinger, V Brovkin,
342 T Crueger, M Esch, K Fieg, et al. Climate and carbon cycle changes from 1850 to
343 2100 in mpi-esm simulations for the coupled model intercomparison project phase 5.
344 *Journal of Advances in Modeling Earth Systems*, 5(3):572–597, 2013.

345 Veit Helm, Angelika Humbert, and Heinrich Miller. Elevation and elevation change of
346 greenland and antarctica derived from cryosat-2. *The Cryosphere*, 8(4):1539–1559,
347 2014.

348 A Hu and C Deser. Uncertainty in future regional sea level rise due to internal climate
349 variability. *Geophysical Research Letters*, 40(11):2768–2772, 2013.

350 JH Jungclaus, N Keenlyside, M Botzet, H Haak, J-J Luo, M Latif, J Marotzke,
351 U Mikolajewicz, and E Roeckner. Ocean circulation and tropical variability in the
352 coupled model echam5/mpi-om. *Journal of climate*, 19(16):3952–3972, 2006.

353 M Perrette, F Landerer, R Riva, K Frieler, and M Meinshausen. A scaling approach
354 to project regional sea level rise and its uncertainties. *Earth System Dynamics*, 4(1):
355 11–29, 2013.

356 A Shepherd, E R Ivins, A Geruo, V R Barletta, M J Bentley, S Bettadpur, K H Briggs,
357 D H Bromwich, Ré Forsberg, N Galin, et al. A reconciled estimate of ice-sheet mass
358 balance. *Science*, 338(6111):1183–1189, 2012.

359 ABA Slangen, M Carson, CA Katsman, RSW van de Wal, A Köhl, LLA Vermeersen,
360 and D Stammer. Projecting twenty-first century regional sea-level changes. *Climatic*
361 *Change*, pages 1–16, 2014.

362 D Stammer. Response of the global ocean to greenland and antarctic ice melting. *Journal*
363 *of Geophysical Research: Oceans (1978–2012)*, 113(C6), 2008.

- 364 D Stammer, N Agarwal, A Köhl, and CR Mechoso. Sea level response to greenland ice
365 melting in a coupled climate model. *Surveys in Geophysics*, 32(3-4):621–642, 2011.
- 366 D Swingedouw, C B Rodehacke, E Behrens, M Menary, S M Olsen, Y Gao,
367 U Mikolajewicz, J Mignot, and A Biastoch. Decadal fingerprints of freshwater
368 discharge around greenland in a multi-model ensemble. *Climate dynamics*, 41(3-4):
369 695–720, 2013.
- 370 R Tailleux, A Lazar, and CJC Reason. Physics and dynamics of density-compensated
371 temperature and salinity anomalies. part i: Theory. *Journal of physical oceanography*,
372 35(5):849–864, 2005.
- 373 K E Taylor, R J Stouffer, and G A Meehl. An overview of cmip5 and the experiment
374 design. *Bulletin of the American Meteorological Society*, 93(4), 2012.
- 375 J van den Berk and SS Drijfhout. A realistic freshwater forcing protocol for ocean-
376 coupled climate models. *Ocean Modelling*, 81:36–48, 2014.

Table 1. Total integrated freshwater discharge due to net mass loss rates from GIS and AIS and basin integrated freshwater content differences averaged for 2081-2099 (in $10^{13}m^3$).

Scenario	Input Freshwater Volume				Integrated Freshwater Differences					
	GIS	AIS	E-P	NET	NA	SA	PAC	IO	AO	SO
RCP4.5	4.5	1.3	0.306	5.91	1.92	-0.69	2.43	-0.18	0.84	2.57
RCP8.5	6.3	0.91	0.901	7.57	4.86	0.25	-1.18	-0.56	0.61	1.89

NET refers to the sum of GIS, AIS and net E-P surface freshwater differences, including differences in run-off. Individual basins over which the freshwater content has been integrated are **NA**:North Atlantic, **SA**: South Atlantic, **PAC**:Pacific, **IO**: Indian Ocean, **AO**: Arctic Ocean, **SO**: Southern Ocean

Table 2. Basin-averaged steric, thermo-steric and halo-steric sea level differences averaged over the period 2081 - 2099 (in cm).

Basin	RCP 4.5			RCP 8.5		
	Steric	Thermo-steric	Halo-steric	Steric	Thermo-steric	Halo-steric
NA	1.848	0.12	1.78	1.78	-1.62	3.51
SA	0.57	1.348	-0.82	0.82	0.51	0.33
PO	0.35	0.07	0.29	0.187	0.402	-0.22
IO	0.41	0.56	-0.17	0.163	0.42	-0.271
AO	2.21	0.40	1.85	1.68	0.084	1.806
SO	0.53	0.09	0.45	0.296	-0.042	0.3472

Individual basins over which the freshwater content has been integrated are **NA**:North Atlantic, **SA**: South Atlantic,**PAC**:Pacific, **IO**: Indian Ocean, **AO**: Arctic Ocean, **SO**: Southern Ocean

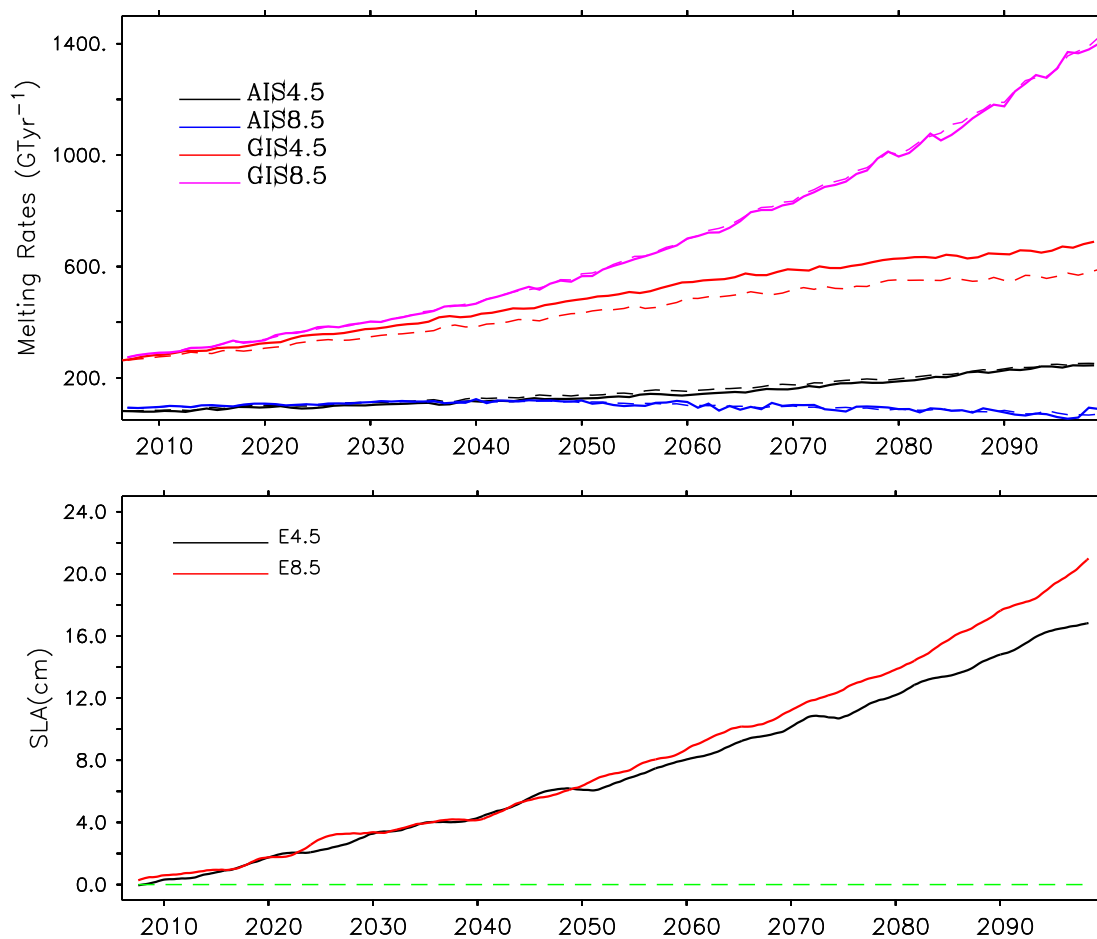


Figure 1. (top) Greenland and Antarctic Ice Sheet mass loss rates (Gyr^{-1}) for RCP 4.5 and RCP 8.5 scenarios, respectively. Dashed lines indicate the corresponding mass loss rates from IPCC AR5 report. (bottom) Differences of low pass filtered global mean sea level (in cm) from (black line) E4.5 and (red line) E8.5. The dashed line in green represents the zero line .

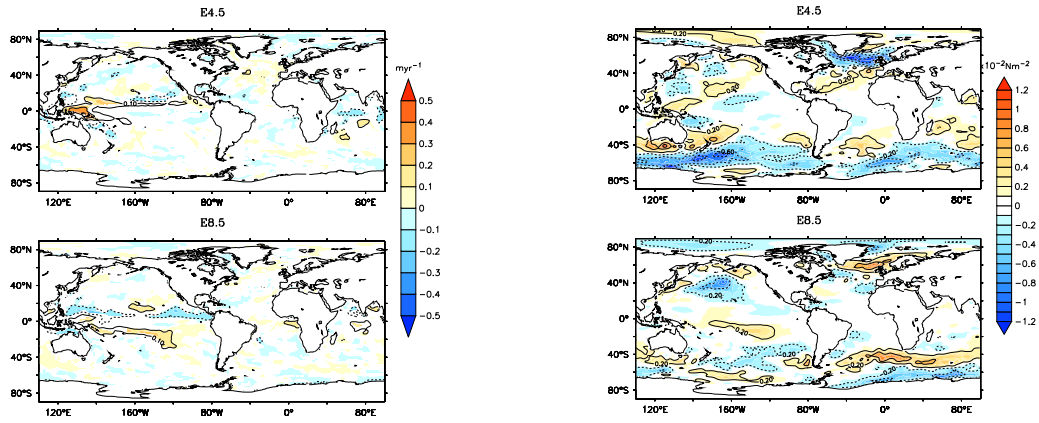


Figure 2. Differences of (left) freshwater fluxes (myr^{-1}) and, (right) zonal wind stress ($\times 10^{-2} \text{Nm}^{-2}$), both averaged over the period 2081-2099 from (top) E4.5 and (bottom) E8.5.

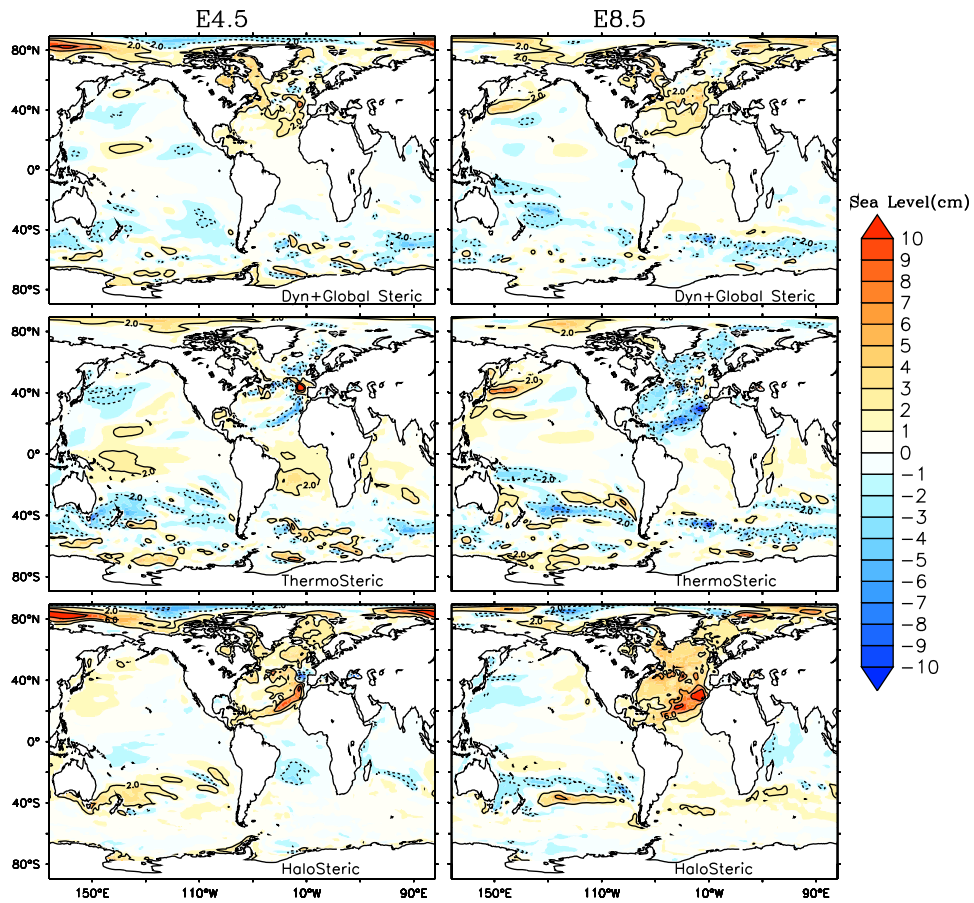


Figure 3. (top) Sea level (cm) change (dynamical + global mean steric) (middle) ThermoSteric and (bottom) halosteric sea level (cm) changes from (left) E4.5 and (right) E8.5 averaged over the period 2081-2099

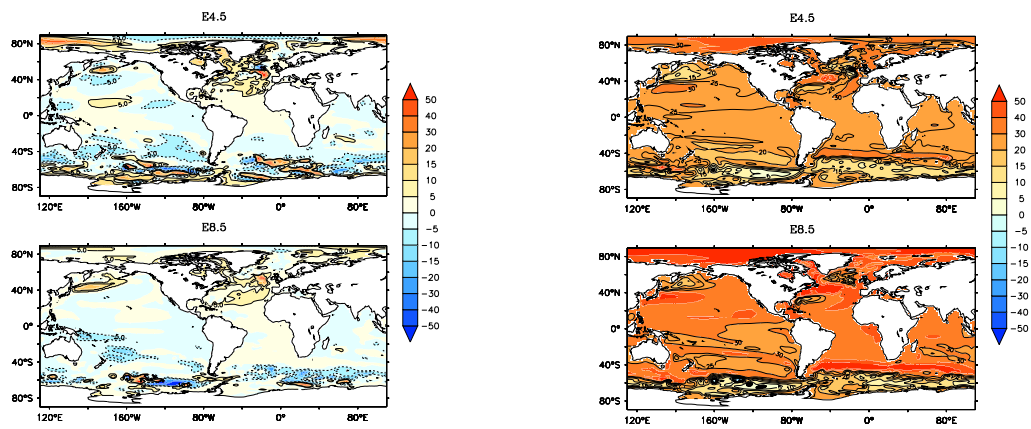


Figure 4. (left) Percentage change in the steric sea level due to net mass loss rates from AIS and GIS for (top) E4.5 and (bottom) E8.5 averaged for the period 2081-2099 after normalization with the respective differences 2081-2099 minus 1986-2005. (right) 3-member ensemble averaged sea level (cm) change from (top) RCP4.5 and (bottom) RCP8.5 standard MPI-ESM CMIP5 reference runs averaged for 2081-2099. The change is computed with reference to sea level averaged over 1986-2005.